Eigenstates and fine structure of a hydrogenic impurity in a spherical quantum dot

Chun-Ching Yang, Li-Chi Liu, and Shih-Hsin Chang
Department of Physics, National ChangHua University of Education, Changhua, Taiwan, Republic of China
(Received 7 October 1997; revised manuscript received 16 March 1998)

The fine structure of the energy levels for a hydrogenic impurity located in the center of a spherical quantum dot is calculated using a simpler exact solution for the potential well. The results reveal that when the dot radius approaches zero, the eigenenergies are just like a free-space hydrogenic atom. When the dot radius is large enough, then the eigenenergies approach a free-space hydrogenic atom but are shifted by the confining potential. Also we find that the radial expectation values will be equal to a free-space hydrogenic atom, when the dot radius is extremely small and extremely large. Between these two situations, the radial expectation values are smaller than those of a free space because of the pressing of the confining potential. Not every dot radius influences the eigenenergy to the same degree. It is decided by the bumps of the electron's wave function and the place of the potential well's margin. When the margin of the well begins to push the bumps of the wave then the eigenenergy will increase more quickly. Because of the changing of the electron distribution probability, the degeneracy of the different l value in a free-space hydrogenic atom is removed by the confining potential. The total-energy shifts of the fine structure of the impurity could be six times larger than the total energy shifts of a free-space atom. [S0163-1829(98)08127-2]

I. INTRODUCTION

Since the technique for understanding the world of nanostructures has improved very much during recent years, we can now detect the fine-structure splitting spectra of a single quantum dot,[1] and people have become more concerned with the quantum effect of low-dimensional systems. Quantum effects of the doping atom caused by the confining potential are predicated to be much different with a normal free-space atom. Many people are interested in studying areas, such as quantum wells (QW), quantum-well wires (QWW), and quantum dots (QD). Bastard[2,3] was the first to work on the binding energy of a hydrogenic impurity in an infinite potential well. Bryant[4] calculated the impurity's binding energy in quantum-well wires by assuming a cylinder coordinate. Parras-Montenegre[5] *et al.* used a variational procedure within the effective-mass approximation to calculate the binding energies of hydrogenic impurity in QD. Zhu *et al.*[6,7] solved the finite potential well for the impurity in the center of the QD and obtained the exact solutions by using the method of series expansion. Chu, Hsiao, and Mei[8] resolved the infinite potential-well equation and presented a detailed formulation for the state energies of the hydrogenic impurity located at the center of the QD and the QW. After that people began to research new problems, such as the off-center impurity,[9] the cubic quantum dot,[10] and others.[11,12] Although much research has been done on various aspects of electronic properties in a nanostructure as mentioned above, however, a simpler convenient exact solution for the spherical QD of the finite potential still has not been found. Although Zhu's solution is quite correct, it is hard to calculate the other expectation values for the impurity by using the solution. Chu has found a good exact solution, but it is only for the infinite potential well. Most of them (Parras-Montenegro, Zhu, and Chu) paid attention to the binding energy of the impurity, but for the eigenstates, the wave function's penetrating situations, radial expectation values and the fine structure of the impurity itself are disregarded.

In this paper we calculate eigenvalues mentioned above and present our calculations and discussions in two sections. In Sec. II, we present a simpler exact solution for the infinite and finite potential well and we discuss how a QD influences the impurity's wave function, radial expectation value, and the other physical expectation quantities. In Sec. III, we use the solutions we calculated to be our zero-order wave functions and calculate the fine structure of the impurity. These are the energy shifts due to the spin-orbit interaction, the relativistic correction to the kinetic energy, and the relativistic correction to the potential energy, which is called the Darwin term. A summary of results is presented in Sec. IV.

II. EIGENSTATES AND RADIAL EXPECTATION VALUES

A. Formulation

The Hamiltonian of a hydrogenic impurity located in the center of a spherical quantum dot (SQD) can be written as

$$H_0=\left[-\frac{\hbar^2}{2\mu}\nabla^2-\frac{KZe^2}{\epsilon r}+V(r)\right], \tag{1}$$

where

$$V(r)=\begin{cases}-V_0, & r<R_0\\ 0, & r\geqslant R_0\end{cases} \tag{2}$$

and μ, K, ϵ, and Z are the effective mass, electrical constant, dielectric constant, and core charge, V_0 and R_0 are the confining potential and the radius of the SQD, and they are all positive. The value of the confining potential V_0 is from zero to infinity. The solution of the Schrödinger equation, because it is a spherical symmetric potential field, can be written as

$$\psi(r,\theta,\Phi)=R(r)Y(\theta,\Phi).$$

We are only concerned with bound states, so the eigenenergies are negative $E=-|E|$, and the differential equation for the radical part $R(r)$ can be written in spherical coordinates. For inside the well $r<R_0$:

$$\frac{\partial^2}{\partial r^2}R(r)+\frac{2}{r}\frac{\partial}{\partial r}R(r)+\frac{2\mu}{\hbar^2}\left(-|E|+V_0+\frac{KZe^2}{\epsilon r}\right)\times R(r)-\frac{l(l+1)}{r^2}R(r)=0; \tag{3}$$

for outside the well $r\geqslant R_0$:

$$\frac{\partial^2}{\partial r^2}R(r)+\frac{2}{r}\frac{\partial}{\partial r}R(r)+\frac{2\mu}{\hbar^2}\left(-|E|+\frac{KZe^2}{\epsilon r}\right)\times R(r)-\frac{l(l+1)}{r^2}R(r)=0. \tag{4}$$

Therefore we can study the solutions of these two equations in two regions. One is the inside region for $r<R_0$, the other one is the outside region for $r\geqslant R_0$.

1. The inside region $r<R_0$

Here we study the inside solution with three cases. Case 1: $|E|<V_0$; case 2: $|E|>V_0$; and case 3: $|E|=V_0$.

Case 1: $|E|<V_0$. For $|E|<V_0$ Eq. (3) is convenient to rescale distances and energies to define dimensionless variables. Therefore we define

$$\rho_<=2\left(\frac{2\mu(V_0-|E|)}{\hbar^2}\right)^{1/2}r,$$

$$\lambda_<=\frac{KZe^2}{\epsilon\hbar}\left(\frac{\mu}{2(V_0-|E|)}\right)^{1/2}.$$

With these definitions, Eq. (3) becomes

$$\frac{\partial^2R(r)}{\partial\rho_<^2}+\frac{2}{\rho_<}\frac{\partial R(r)}{\partial\rho_<}-\frac{l(l+1)}{\rho_<^2}R(r)+\left(\frac{\lambda_<}{\rho_<}+\frac{1}{4}\right)R(r)=0. \tag{5}$$

This is similar to the free-electron equation of the hydrogen atom. It has two complex conjugated solutions.[13] The first one is the outgoing wave:

$$R(r)^{(+)}=e^{+i\rho_</2}\rho_<^lM(l+1-i\lambda_<,2l+2,-i\rho_<). \tag{6}$$

The second one is the incoming wave:

$$R(r)^{(-)}=e^{-i\rho_</2}\rho_<^lM(l+1+i\lambda_<,2l+2,+i\rho_<), \tag{7}$$

where M is the confluent hypergeometric function:

$$M(a,b,X)=\sum_{n=0}^{\infty}\frac{(a)_nX^n}{(b)_nn!}.$$

Although we use the hydrogenic free-electron solution for the equation, the electron is still confined in the potential. It can be totally reflected. The wave function must contain waves in both directions. So the general solution is

$$R(r)=AR(r)^{(+)}+BR(r)^{(-)}.$$

Since the reflection coefficient must be equal to one, and because of the boundary condition of SQD, we have $A=B$. The value of $\lambda_<$ can be determined from boundary conditions. The eigenenergies of the impurity may be given as

$$E_{\lambda_<l}=-\left(V_0-\frac{\mu K^2Z^2e^4}{2\epsilon^2\hbar^2\lambda_<^2}\right). \tag{8}$$

Case 2: $|E|>V_0$. For $|E|>V_0$, we define new variables for Eq. (3):

$$\rho_>=2\left(\frac{2\mu(|E|-V_0)}{\hbar^2}\right)^{1/2}r,$$

$$\lambda_>=\frac{KZe^2}{\varepsilon\hbar}\left(\frac{\mu}{2(|E|-V_0)}\right)^{1/2},$$

with these new definitions we rewrite Eq. (3) as follows:

$$\frac{\partial^2R(r)}{\partial\rho_>^2}+\frac{2}{\rho_>}\frac{\partial R(r)}{\partial\rho_>}-\frac{l(l+1)}{\rho_>^2}R(r)+\left(\frac{\lambda_>}{\rho_>}-\frac{1}{4}\right)R(r)=0. \tag{9}$$

The solution is similar to the equation of hydrogen with a bound electron:

$$R(r)=e^{-\rho_>/2}\rho_>^l\sum_{n=0}^{\infty}a_n\rho_>^n. \tag{10}$$

The recursion relation is

$$a_{n+1}=\frac{n+l+1-\lambda_>}{(n+1)(n+2l+2)}a_n \quad\text{and}\quad a_0=1. \tag{11}$$

Again by matching the boundary conditions we can find the value of $\lambda_>$, and the eigenenergies may be given as

$$E_{\lambda_>l}=-\left(V_0+\frac{\mu K^2Z^2e^4}{2\varepsilon^2\hbar^2\lambda_>^2}\right).$$

Case 3: $|E|=V_0$. As $|E|=V_0$ Eq. (3) becomes

$$\left[\frac{\partial^2}{\partial r^2}+\frac{2}{r}\frac{\partial}{\partial r}-\frac{l(l+1)}{r^2}\right]R(r)-\frac{2\mu}{\hbar^2}\frac{KZe^2}{\varepsilon r}R(r)=0. \tag{12}$$

We can search for a solution of the form, such as

$$R(r)=r^s\sum_n^{\infty}a_nr^n. \tag{13}$$

Now substitute the power-series expansion for $R(r)$. This gives the solution

$$s=l$$

and

$$a_{n+1}=\frac{-(2\mu/\varepsilon\hbar^2)KZe^2}{(n+2l+2)(n+1)}a_n \quad\text{with}\quad a_0=1.$$

For an impurity in SQD there is probably no eigenstate whose energy is equal to V_0. If there was, then there would be only one state that we could find for $|E|=V_0$.

2. The outside region $r \geqslant R_0$

Here we define new variables for the outside region for Eq. (4):

$$\rho_{\text{out}} = 2\left(\frac{2\mu|E|}{\hbar^2}\right)^{1/2} r,$$

$$\lambda_{\text{out}} = \frac{KZe^2}{\varepsilon\hbar}\left(\frac{\mu}{2|E|}\right)^{1/2}.$$

Then Eq. (4) can be rewritten as follows:

$$\frac{\partial^2 R(r)}{\partial \rho_{\text{out}}^2} + \frac{2}{\rho_{\text{out}}}\frac{\partial R(r)}{\partial \rho_{\text{out}}} - \frac{l(l+1)}{\rho_{\text{out}}^2} R(r) + \left(\frac{\lambda_{\text{out}}}{\rho_{\text{out}}} - \frac{1}{4}\right) R(r) = 0. \tag{14}$$

In order to find a solution in which the probability of finding the electron at very large distances from the center of the field must go to zero, we derive a general solution of Eq. (14) as follows:

$$R(r) = e^{-\rho_{\text{out}}/2} \rho_{\text{out}}^{-s} \sum_{n=0}^{\infty} a_n \rho_{\text{out}}^{-n}. \tag{15}$$

By substituting the solution into Eq. (14), we get s and the recursion relation

$$s = l - \lambda_{\text{out}},$$

$$a_{n+1} = \frac{-(n+l+1-\lambda_{\text{out}})(n-1-\lambda_{\text{out}})}{(n+1)} a_n.$$

This solution is an asymptotic series solution.[14]

B. Discussion

By imposing the solutions to the boundary conditions we can get a suitable λ value for every state of the impurity, and the λ values for each state need not be integers. From it we can find out the hydrogenic impurity's eigenenergies, wave functions, and radial expectation values. To make our results more understandable, we let the reduced mass and the dielectric constant be the same with a free-space hydrogen, that is, the effective Rydberg energy R_y^* is equal to Rydberg energy R_y (13.6 eV), and effective Bohr radius a^* is equal to Bohr radius a_0 (0.529 Å). Here we assume that the confining potential V_0 is 5 eV. For convenience, we still use the principal number n to represent the eigenstate in order to compare with the corresponding states of a free-space hydrogen. In Figs. 1 and 4 below, the negative scale of the y axis is related only to the wave function. It is not related to the drawing of the confining potential. The confining potential is related only to the x axis. The results are as follows:

In Fig. 1, we present the $4f$ wave function as a function of the dot radius. It is apparent that when the dot radius is extremely large then the confining potential has a very small influence on the impurity, and the wave function approaches the corresponding state of a free-space hydrogen atom. In Fig. 1(a), as the dot radius decreases, the wave function is pushed into the inner space of the impurity by the confining well. In Fig. 1(b), while the dot radius continuously decreases, the wave function penetrates into the outside region of the quantum dot more and more. The eigenenergy of the bound state becomes larger and larger. During this time we can see the wave function transferring from the inside to the outside region of the well, and the wave function is widely spread in a large domain, as in the electron radial probability distribution. In Fig. 1(c), when the size of SQD is extremely small, it is apparent that the wave function approaches the free-space hydrogen again, and most of the wave exists at the outside region of the confining well, and the wave function distributes itself at a region that is similar to the wave function of a free-space hydrogen atom.

In Fig. 2, we present the eigenenergies of different n l states as a function of the dot radius. (l is orbital quantum number.) For each n state, the eigenenergy increases as the radius decreases. It is found that when the dot radius is extremely small the eigenenergies $E_{\lambda l}$ of the impurity approach the corresponding energies of a free-space hydrogen: $E \cong -Z^2 R_y^*/n^2$. And when the dot radius is large enough, the eigenenergy approaches a value that is equal to the confining potential plus the corresponding energy of a free-space hydrogen: $E \cong -(Z^2 R_y^*/n^2 + V_0)$. Also when the dot radius is at these two extreme situations, eigenenergies are in l degeneracy as the degeneracy of a free-space hydrogen atom.

Between these two extreme situations, the l degeneracy disappears. For the same principal number, when the dot radius decreases, the smaller l states' eigenenergies increase more quickly than the bigger l states. Because when the confining electron is in a small l state, most of time it distributes itself at the more outer part of the impurity than the electron in big l state. While the dot radius is decreasing, the margin of the confining potential pushes the small l state first. So its eigenenergy is influenced earlier than the big l state. That is why the small l state's energy increases quicker than the big l state as the dot radius decreases.

The number of times that the energy increases is equal to the bump number of the electron radial probability distribution function. For example, since there are two bumps in the radial probability distribution function of the $2s$ state, therefore the $2s$ state's eigenenergy has two increasing times as the dot radius decreases from $35a_0$ to zero. The reason is that when the margin of the well meets the outer bump, then it will push the bump into the inner part of the impurity. During this time the influence of the well is apparent, and so the eigenenergy increases more quickly. When the outer bump has penetrated the well, then the node of the function is near the well's margin. During this time the eigenenergy increases slowly, and the changes of the dot radius seem to have little influence on the impurity. But when the margin meets the inner bump and begins to push the bump, the eigenenergy increases quickly again. We found that not every dot radius influences the eigenenergy apparently. It depends on which state the confining electron is in and what the value of the dot radius is. Also we can see from the figure that there is no critical dot radius for which we could not find any bound state, because the potential of the impurity is not a square well potential. It is proportional to r^{-1} at the outside region of the SQD, and this is why there is no critical dot radius.

In Fig. 3, we present radial expectation values of the $4f$ state as the function of the dot radius. We can see that the radial expectation values are consistent with the wave func-

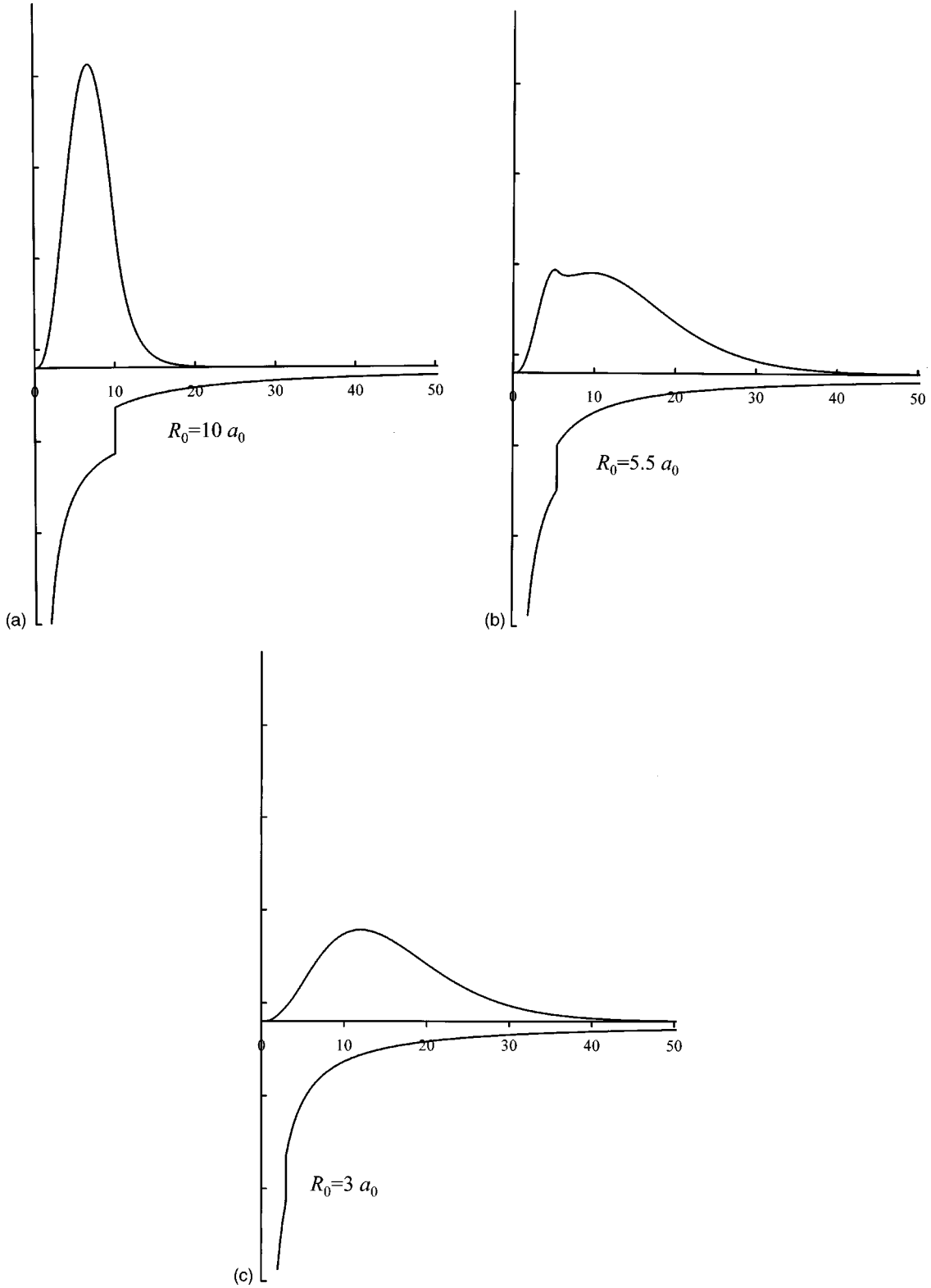

FIG. 1. The $4f$ state wave function of a hydrogenic impurity in the center of SQD of 5 eV well depth is expressed as a function of the impurity's radius with three different dot radii. At the bottom of each picture, in order to have a better understanding, we plot the confining potential well.

tions of the $4f$ state in Fig. 1. When the dot radius is large ($60a_0$), the expectation value approaches the value of a free-space hydrogen, because the confining potential has few influences on the impurity. When the dot radius decreases, the margin of the confining potential begins to push the electron into the inner region of the impurity, so the radial expectation values become smaller and smaller. Finally they reach a limit, and when the wave function begins to penetrate out of the margin of the SQD, the radial expectation value begins getting larger. At the same time, the eigenenergy is also get-

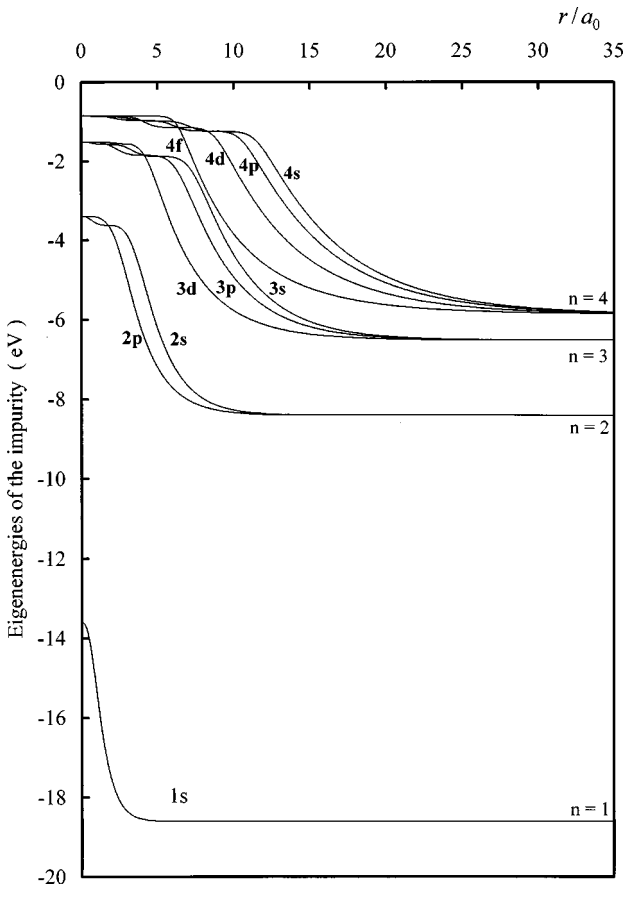

FIG. 2. The eigenenergies of a hydrogenic impurity in the center of a SQD of 5 eV well depth, from $1s$ to $4f$ states is expressed as a function of the dot radius.

ting larger. As the dot radius is extremely small, most of the wave function exists at the outside region of the dot. Then the radial expectation value approaches the value of a free-space hydrogen again.

In Fig. 4, we show the $5s$ state's wave function. By using the solutions we mentioned above, we can still find out the exact wave function for the impurity. There is no limiting value of the dot radius for which we can not find the bound state.

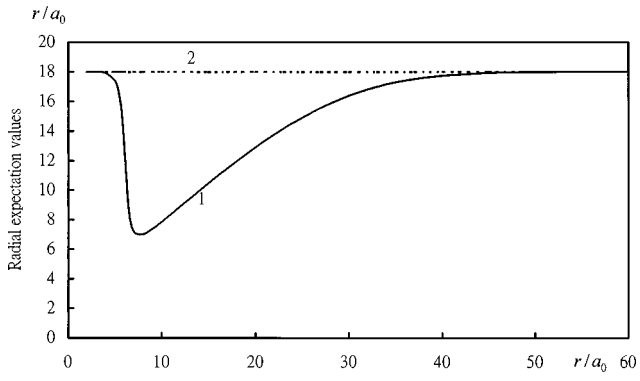

FIG. 3. The $4f$ state's radial expectation value of a hydrogenic impurity in a SQD of 5 eV well depth is expressed as a function of the dot radius (curve 1). The curve 2 represents a radial expectation value of a free-space hydrogen.

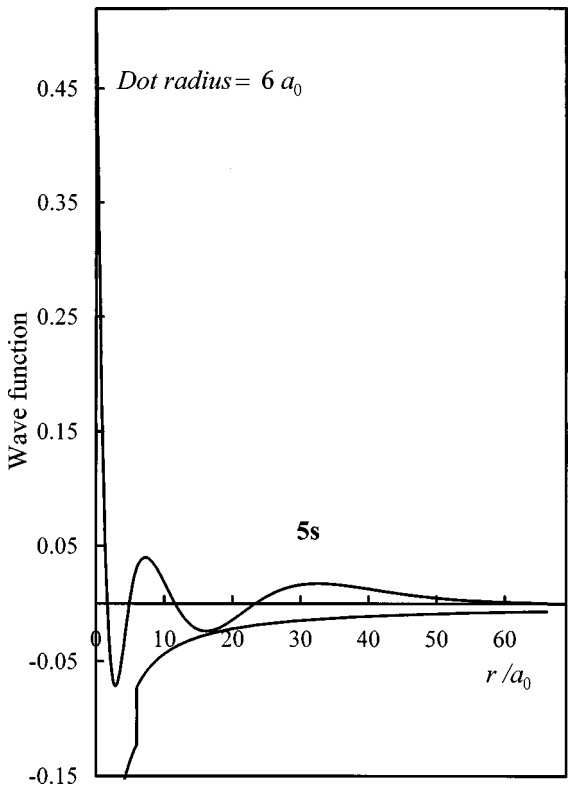

FIG. 4. The $5s$ state wave function for the impurity is expressed as the function of the impurity radius. And the function of the confining potential.

III. THE FINE STRUCTURE OF THE IMPURITY

A. Formulation

The Hamiltonian for the fine-structure calculation can be written as

$$H = H_0 + H'.$$

The unperturbed Hamiltonian H_0 is the same as Eq. (1). The perturbation H' is given as[15]

$$H' = H_1' + H_2' + H_3',$$

with

$$H_1' = \left(\frac{KZe^2}{\varepsilon}\right) \frac{1}{2m^2c^2r^3}\, \mathbf{S}\cdot\mathbf{L},$$

$$H_2' = \frac{-P^4}{8m^3c^2}$$

and

$$H_3' = \frac{\pi\hbar^2}{2m^2c^2}\left(\frac{KZe^2}{\varepsilon}\right)\delta(r), \tag{16}$$

where the first term, H_1', is the spin-orbit term, the second term, H_2', is the relativistic correction to the kinetic energy and the third term, H_3', is the Darwin term. We shall start from the unperturbed term equation

$$H_0\psi_{\lambda l m_l m_s} = E_{\lambda l}\psi_{\lambda l m_l m_s} \tag{17}$$

with

$$\psi_{\lambda l m_l m_s}=\psi\lambda l m_l \chi_{1/2,m_s}=R_{\lambda l}(r)Y_{lm_l}(\theta,\phi)\chi_{1/2,m_s},$$

where $\psi_{\lambda l m_l m_s}$ is the zero-order wave function of the unperturbed state and the $R_{\lambda l}(r)$ is the radial function we calculated in Sec. II.

When we calculate the fine structure of the impurity, we use the time-independent perturbation theory for the impurity's energy levels. Here we calculate the first-order energy correction to the energy levels $E_{\lambda l}$ due to the terms H_1', H_2', and H_3'.

1. Energy shift due to the term H_1' (spin-orbit term)

Since the perturbation H_1' is diagonal in the couple $\psi_{\lambda l j m_j}$ representation, we construct the functions $\psi_{\lambda l j m_j}$ from linear combinations of functions $\psi_{\lambda l m m_s}$. We obtain

$$\psi_{\lambda l j m_j}=\sum_{m_l m_s}\langle l s m_l m_s|j m_j\rangle\psi_{\lambda l m_l m_s},$$

where $\langle l s m_l m_s|j m_j\rangle$ are Clebsch-Gordan coefficients. So we have the first-order energy correction ΔE_1 due to H_1' as

$$\begin{aligned}\Delta E_1&=\langle\psi_{\lambda' l' j' m_j'}|H_1'|\psi_{\lambda l j m_j}\rangle\\&=\delta_{ll'}\delta_{m_j m_j'}\delta_{jj'}\left(\frac{KZe^2}{\epsilon}\right)\frac{1}{4m^2c^2}\left\langle\frac{1}{r^3}\right\rangle_{\lambda l}\\&\quad\times\hbar^2\left[j(j+1)-l(l+1)-\frac{3}{4}\right],\end{aligned}\tag{18}$$

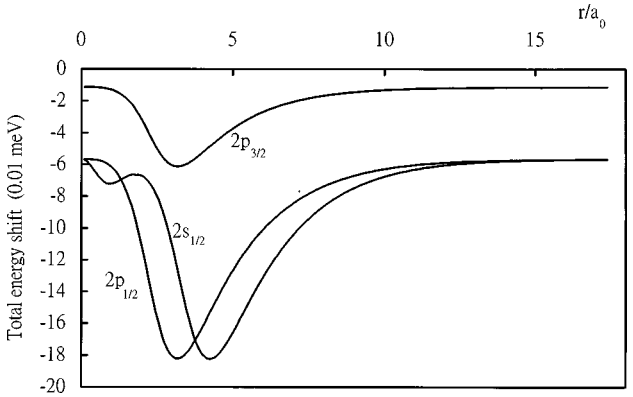

FIG. 5. Total energy shifts of $2s_{1/2}$, $2p_{1/2}$, and $2p_{3/2}$, as the function of the dot radius.

where

$$j=\begin{cases}l\pm\frac{1}{2}, & l\neq 0\\ \frac{1}{2}, & l=0.\end{cases}$$

2. Energy shift due to the term H_2' (relativistic correction to the kinetic energy)

For calculating the energy shift due to H_2', we rewrite this term as

$$H_2'=\frac{-p^4}{8m^3c^2}=-\frac{1}{2mc^2}\left[H_0+\frac{KZe^2}{\varepsilon r}-V(r)\right]^2.$$

The first-order energy correction ΔE_2 due to H_2' is given by

$$\begin{aligned}\Delta E_2=\langle\psi_{\lambda l m_l m_s}|H_2'|\psi_{\lambda l m_l m_s}\rangle=&-\frac{1}{2mc^2}\left[E_{\lambda l}^2+2E_{\lambda l}\frac{KZe^2}{\varepsilon}\left\langle\frac{1}{r}\right\rangle_{\lambda l}+\frac{K^2Z^2e^4}{\varepsilon^2}\left\langle\frac{1}{r^2}\right\rangle_{\lambda l}+V_0^2\int_0^{R_0}R_{\lambda l}^2r^2dr\right.\\&\left.+2E_{\lambda l}\int_0^{R_0}R_{\lambda l}^2V_0r^2dr+\frac{2KZe^2V_0}{\varepsilon}\int_0^{R_0}R_{\lambda l}^2\left(\frac{1}{r}\right)r^2dr\right].\end{aligned}\tag{19}$$

3. Energy shift due to the term H_3' (Darwin term)

This term acts only at the origin, for since the case $l\neq 0$ the wave functions of the impurity vanish at $r=0$, we only have to consider the case $l=0$. Because H_3' does not act on the spin variable and commutes with the operators $\mathbf{L}^2$ and $\mathbf{L}_Z$, it is also diagonal in the matrix. The energy shift ΔE_3 due to the H_3' is given by

$$\begin{aligned}\Delta E_3&=\frac{\pi\hbar^2}{2m^2c^2}\left(\frac{KZe^2}{\varepsilon}\right)\langle\psi_{\lambda 00}|\,\delta(r)\,|\psi_{\lambda 00}\rangle\\&=\frac{\pi\hbar^2}{2m^2c^2}\left(\frac{KZe^2}{\varepsilon}\right)\frac{1}{4\pi}\,|R_{\lambda 0}(0)|^2.\end{aligned}\tag{20}$$

B. Discussion

Here we have calculated the fine structure of the $n=2$ state for the impurity and present them below as a function of the radius of the SQD. In Fig. 5, we present the total-energy shift $\Delta E=\Delta E_1+\Delta E_2+\Delta E_3$ as a function of the dot radius. The upper curve represents the total-energy shift of the $2p_{3/2}$. Two curves in the lower part of the figure are the total energy shifts of $2p_{1/2}$ and $2s_{1/2}$ in which both j values are the same. In the impurity, the total-energy shift of the impurity not only depends on the j value, it also depends on the l value. We can see that the energy shifts $2p_{1/2}$ and $2s_{1/2}$ are different in a dot radius. The reason is that the total-energy shift ΔE depends on the expectation values of $\langle 1/r\rangle$, $\langle 1/r^2\rangle$, and $\langle 1/r^3\rangle$. They are all l dependent because of the l dependency of the electron probability distribution, which is influenced by the SQD. That is why the degeneracy $2p_{1/2}-2s_{1/2}$ of the energy shift is removed by the quantum dot. But when the dot radius is in an extreme situation, very small or large, the total-energy shifts approach that of a free-space hydrogen atom, and the total energy shifts of $2p_{1/2}$ and $2s_{1/2}$

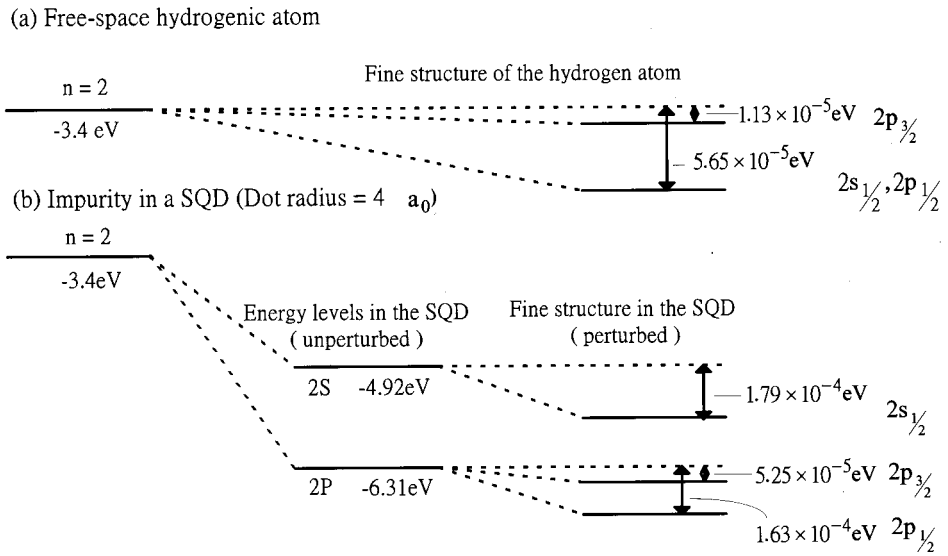

FIG. 6. Fine structure of the free-space hydrogen atom and the impurity. For clarity, the scale in each diagram is different.

get close to each other, then the degeneracy of these two states is recurs. Also we can see that, when the dot radius is between $3a_0$ and $5a_0$, the total-energy shift of the impurity could be about six times larger than that of a free-space atom. They are apparently influenced by the SQD.

In Fig. 6, we plot two fine-structure splitting diagrams. In Fig. 6(a), we present the fine structure of a free-space hydrogen atom when $n=2$, in order to compare it with the impurity. We can see that the fine structure $2p_{1/2}-2s_{1/2}$ of the free-space atom is degenerate. In Fig. 6(b) we present the fine-structure splitting of the $n=2$ state of the impurity in a SQD with dot radius $R_0=4a_0$. When the impurity is doped in a SQD, the $n=2$ state splits into two energy levels, $2s$ and $2p$, which we call the unperturbed energy levels. After the fine structure is taken into account the spin degeneracy is removed, and they split into three energy levels, $2s_{1/2}$, $2p_{1/2}$, and $2p_{3/2}$, which we call perturbed energy levels.

In Table I, we list some values of the unperturbed energy values and the energy shifts of $n=2$ state for different dot radii. We can see that when the dot radius is extremely large ($R_0=17a_0$) or small ($R_0=0.1a_0$) the energy shifts approach to the value of a free-space hydrogen. The reasons are discussed in Sec. II.

IV. CONCLUSION

We derived a simpler exact solution for a hydrogenic impurity located at center of a quantum dot and calculated the fine structure of the impurity. We found that as the dot radius becomes very large, the energy levels approach the corresponding states of a free-space hydrogen atom, but are shifted by the confining potential V_0. As the dot radius becomes very small, there still are bound states similar with the corresponding states of a free-space hydrogen. Between these two limitations the energy levels increase from $E=-(Z^2R_y^*/n^2+V_0)$ to $E=-Z^2R_y^*/n^2$. Also we find the number of times that the energy increases is equal to the number of bumps of the radial probability distribution function. As far as the radial expectation values are concerned, they are smaller than those of a free-space hydrogenic atom,

TABLE I. Energy values and shifts of each state of an impurity in SQD with different dot radii. The unit of $E_{\lambda l}$ is in electron volts (eV), and units of ΔE_1, ΔE_2, ΔE_3, and ΔE are in 0.01 meV.

		$E_{\lambda l}$	ΔE_2	ΔE_1	ΔE_3	ΔE
	$2s_{1/2}$	−3.402	−14.8	0	9.11	−5.70
$R_0=0.1$	$2p_{1/2}$	−3.401	−2.65	−3.03	0	−5.68
	$2p_{3/2}$	−3.401	−2.65	1.51	0	−1.14
	$2s_{1/2}$	−4.923	−40.8	0	22.9	−17.9
$R_0=4.0$	$2p_{1/2}$	−6.306	−8.92	−7.33	0	−16.3
	$2p_{3/2}$	−6.306	−8.92	3.67	0	−5.25
	$2s_{1/2}$	−7.990	−21.8	0	13.2	−8.62
$R_0=8.0$	$2p_{1/2}$	−8.190	−3.57	−3.80	0	−7.37
	$2p_{3/2}$	−8.190	−3.57	1.90	0	−1.67
	$2s_{1/2}$	−8.400	−14.8	0	9.09	−5.67
$R_0=17.0$	$2p_{1/2}$	−8.400	−2.66	−3.03	0	−5.68
	$2p_{3/2}$	−8.400	−2.66	1.51	0	−1.14

but they approach the value of a free-space hydrogen atom when the dot radius is very large or very small. There is no critical dot radius for the bound state, when the dot radius is small, the penetration becomes very large. The result of fine structure reveals that the remaining degeneracy in j is removed by the SQD, and the total energy shifts of the fine structure of the impurity could be six times larger than the total energy shifts of a free-space hydrogen atom.

From our results, by using the effective-mass approximation method, we can understand the fine-structure splitting of an exciton in a single quantum dot. Also by using our solution we can calculate the Zeeman effect, Stark effect, and two-electron confined atoms. These are in progress.

ACKNOWLEDGMENTS

We are grateful to J. L. Chen for many fruitful discussions and suggestions. This work was supported by National Science Council, Taiwan, Republic of China.

[1] D. Gammon, E. S. Snow, B. V. Shanabrook, D. S. Katzer, and D. Park, Phys. Rev. Lett. **76**, 3005 (1996).
[2] G. Bastard, Phys. Rev. B **24**, 4714 (1981).
[3] G. Bastard, E. E. Mendez, L. L. Chang, and L. Esaki, Phys. Rev. B **26**, 1974 (1982).
[4] Garnett W. Bryant, Phys. Rev. B **29**, 6632 (1984).
[5] N. Porras-Montenegro and S. T. Perez-Merchancano, Phys. Rev. B **46**, 9780 (1992).
[6] J. L. Zhu, Phys. Rev. B **39**, 8780 (1989).
[7] J. L. Zhu, J. J. Xiong, and B. L. Gu, Phys. Rev. B **41**, 6001 (1990).
[8] D. S. Chu, C. M. Hsiao, and W. N. Mei, Phys. Rev. B **46**, 3898 (1992).
[9] J. L. Zhu and Xi Chen, Phys. Rev. B **50**, 4497 (1994).
[10] F. J. Ribeiro and A. Latge', Phys. Rev. B **50**, 4913 (1994).
[11] B. Stebe, E. Assaid, F. Dujardin, and S. Le Goff, Phys. Rev. B **54**, 17 785 (1996).
[12] Zhen-Yan Deng, Jing-Kun Guo, and Ting-Rong Lai, Phys. Rev. B **50**, 5736 (1994).
[13] See, for example, Wu and Ohmura, *Quantum Theory of Scattering* (Prentice-Hall, New York, 1962), Chap. 1.
[14] See, for example, George B. Arfken and Hanns J. Weber, *Mathematical Method for Physicists*, 4th ed. (Academic Press, New York, 1995), Sec. 5.10.
[15] See, for example, B. H. Bransden and C. J. Joachain, *Introduction to Quantum Mechanic* (John Wiley & Sons, New York, 1990), Chap. 8.